TECHNICAL REPORT STANDARD PAGE

1. Report No. FHWA/LA-91/246	2. Government Accession No.	3. Recipient's Catalog No.
4. Title and Subtitle EVALUATION OF THE LULING BRIDGE RETROFIT DETAILS UNDER SERVICE LOADS	5. Report Date AUGUST 1991 6. Performing Organization Code	
7. Author(s) Ben T. Yen, Zuo Zhang Ma, Daniel Moser, John W. Fisher	8. Performing Organization Report No.	
9. Performing Organization Name and Address Advanced Technology for Large Structural Systems Lehigh University Bethlehem, PA 18015	10. Work Unit No. 11. Contract or Grant No. La. HPR Study No. 87-2ST	
12. Sponsoring Agency Name and Address Louisiana Department of Transportation & Development Louisiana Transportation Research Center 4101 Gourrier Ave Baton Rouge, LA 70808	13. Type of Report and Period Covered Final Report September 1986, June 1991 14. Sponsoring Agency Code	

15. Supplementary Notes

Conducted in cooperation with the U.S. Department of Transportation, Federal Highway Administration.

16. Abstract

Extensive strain measurements were carried out on three cross girder boxes used to connect the cable stays to the orthotropic deck-trapezoidal box steel structure. The measurements were obtained at CG3, GG4 and CG5 adjacent to the tower at pier 2.

The measurements were focused on details which had known cracks that had been retrofitted by installing holes in the trapezoidal box girder webs at the crack tip. The hole placement resulted in several residual uncracked web segments. These uncracked segments could be modeled for crack growth based on measured stress histories and compared with field observations of crack extension.

The strain gages were installed in October 1986. The gages were protected and connected to junction boxes accessible from the bridge deck. Two types of stress measurements were acquired. On November 4, 1986 two test trucks with known weights of 80,140 pounds and 82,180 pounds were used to obtain the structural response as they traveled across the bridge either side-by-side in two lanes or in tandem in the traveling lane. Test runs were made in the southbound and northbound directions at a crawl speed of about 5 mph and at 60 mph.

In addition, measurements were made under regular truck traffic for the four day period from November 3 to November 6, 1986 using a magnetic tape recorder for continuous analog records. The frequency of trucks was low as only light traffic used the bridge. The measured maximum stress range at the details with cracks varied from 0.1 ksi to 0.74 ksi. These levels of stress range did not appear to exceed the crack growth threshold. Hence no crack extension would develop from the truck traffic using the structure.

During the measurements over 15-1/3 hours, a single large stress range excursion occurred at CG5. The maximum stress range was 16.3 ksi at one of the retrofit holes. It was hypothesized that this resulted from a wind gust and/or an unknown structural release.

Because of the low live load response and single high stress event, no additional measurements were deemed desirable until the connecting roadways are completed and much higher traffic frequency develops.

17. Key Words Cable-stayed steel box girder bridge, crack retrofit, strain measurements, load and traffic stress		18. Distribution Statement No restriction. This document is available to the public through the National Technical Information Services, Springfield, VA 22161.	
19. Security Classif. (of this report) Unclassified	20. Security Classif. (of this page) Unclassified	21. No. of Pages	22. Price

Form DOT F1700.7 (1-92)

EVALUATION OF THE LULING BRIDGE RETROFIT DETAILS UNDER SERVICE LOADS

FINAL REPORT

By

Ben T. Yen, Ph.D.
Professor of Civil Engineering

Zuozhang Ma, M.S.
Research Engineer (Visiting)

Daniel Moser, M.S.
Research Assistant

John W. Fisher, Ph.D., P.E.
Professor of Civil Engineering

ADVANCED TECHNOLOGY FOR LARGE STRUCTURAL SYSTEMS
LEHIGH UNIVERSITY
BETHLEHEM, PA 18015

Conducted For

LOUISIANA DEPARTMENT OF TRANSPORTATION AND DEVELOPMENT
LOUISIANA TRANSPORTATION RESEARCH CENTER
in Cooperation with
U.S. Department of Transportation
FEDERAL HIGHWAY ADMINISTRATION

August 1991

ACKNOWLEDGEMENTS

The study was sponsored by the LaDOTD and the U.S. Department of Transportation Federal Highway Administration. The sponsorship is sincerely appreciated. Thanks are due the LaDOTD for its assistance during this study.

ABSTRACT

Extensive strain measurements were carried out on three cross girder boxes used to connect the cable stays to the orthotropic deck-trapezoidal box steel structure. The measurements were obtained at CG3, GG4 and CG5 adjacent to the tower at pier 2.

The measurements were focused on details which had known cracks that had been retrofitted by installing holes in the trapezoidal box girder webs at the crack tip. The hole placement resulted in several residual uncracked web segments. These uncracked segments could be modeled for crack growth based on measured stress histories and compared with field observations of crack extension.

The strain gages were installed in October 1986. The gages were protected and connected to junction boxes accessible from the bridge deck. Two types of stress measurements were acquired. On November 4, 1986 two test trucks with known weights of 80,140 pounds and 82, 180 pounds were used to obtain the structural response as they traveled across the bridge either side-by-side in two lanes or in tandem in the traveling lane. Test runs were made in the southbound and northbound directions at a crawl speed of about 5 mph and at 60 mph.

In addition, measurements were made under regular truck traffic for the four day period from November 3 to November 6, 1986 using a magnetic tape recorder for continuous analog records. The frequency of trucks was low as only light traffic used the bridge. The measured maximum stress range at the details with cracks varied from 0.1 ksi to 0.74 ksi. These levels of stress range did not appear to exceed the crack growth threshold. Hence no crack extension would develop from the truck traffic using the structure.

During the measurements over 15-1/3 hours, a single large stress range excursion occurred at CG5. The maximum stress range was 16.3 ksi at one of the retrofit holes. It was hypothosized that this resulted from a wind gust and/or an unknown structural release.

IMPLEMENTATION STATEMENT

The strain measurements from truck traffic demonstrated that current truck frequency was small and the magnitude of cyclic stress too little to cause fatigue crack extension of the known uncracked segments.

A single stress event was detected during the 15-1/3 hours of observation. This event was due to unknown causes.

The observed conditions indicate that no further measurements should be made until the connector roads are completed and significant increases in truck traffic occur.

With the low levels of traffic and small magnitudes of cyclic stress, no crack extension is expected under these conditions. Until this condition is changed, it does not warrant special measurement of crack length at the uncracked ligaments nor additional stress range measurements.

Inspections need not be more frequent than required by the biannual inspections.

TABLE OF CONTENTS

LIST OF TABLES

LIST OF FIGURES

LIST OF FIGURES (CONT'D)

LIST OF FIGURES (CONT'D)

LIST OF FIGURES (CONT'D)

1. INTRODUCTION

The Luling Bridge is a cable-stayed box girder bridge over the Mississippi River between Luling and Destrehan, Louisiana. It is a portion of Route I310, which connects Interstate 10 and U.S. 90. The bridge is composed of two longitudinal steel trapezoidal box girders with an orthotropic deck. The box girders are 14 feet deep, 10 feet wide at the bottom, 20.5 feet wide at the top, and 39 feet apart, center to center. The spans are 508 feet, 1222 feet and 495 feet with approach spans at both ends.

The cables of the bridge are attached to two towers and cross girders. Figure 1.1 shows the locations of the cross girders, and the relative position of the cross girders with respect to the longitudinal girders. At the cross girders, the trapezoidal boxes were split into two half sections (upper and lower), longitudinally, so that the cross girders could be bolted in place.

During construction, cracks were discovered in the webs of the trapezoidal box girder at several details at cross girder locations. The details have been designated as "a", "b", "c" and "d", as shown in Figure 1.2 and 1.3. Details "a" and "b" are shown in more detail in Figure 1.4. Examination and evaluation of these cracked details and core samples were made[1], and coring out the web plate at the cracks to create a crack arrest hole was adopted as the method of retrofit.

The purpose of this study is to investigate the effectiveness of the drilled holes in arresting the cracks in the trapezoidal box girder webs. The stresses at or near these holes were measured to determine whether the web plates are still susceptible to crack growth. In this report, the strain gage locations and the procedure of testing, the resulted stresses, the evaluation of residual cracks at cross girder connections, and recommendations for future action are given. The field measurements were made on November 3 to 6, 1986.

2. INSTRUMENTATION AND PROCEDURE OF TESTING

2.1 Strain Gage Locations

Electrical resistance strain gages were attached to the webs of the we trapezoidal box at cross girders CG3, CG4 and CG5 (see Figure 1.1 for designatio All strain gages were inside the box girder. Most of these gages were at the crac arresting holes; a few were placed at the webs and bottom flange plates of t longitudinal box in transverse cross sections. The latter strain gages were used f detecting the response of the box girder to service loads.

The locations of the cracked details were identified by an alphanumeric syste prior to this study. This identification system was maintained in the study, and revealed in Figures 1.1 to 1.4. When two or more strain gages were placed at a deta the locations were designated by top or bottom (T or B), or numerically. Furthermo the strain gages were also numbered for simplicity during testing. Tables 2.1 to 2. summarize the gage identification and numbers. Figures 2.1 to 2.25 depict t location of these gages.

There were a total of 59 strain gages; 24 at CG3, 21 at CG4 and 14 at CG

The strain gages were attached to the steel plates by epoxy adhesive, a connected by insulated cables to three junction boxes outside the box girder. Figu 2.26 shows a gage cable being connected. Figure 2.27 shows gages 20, 21, and (BA8A1-a-T, BA8A1-b-T and BA8A1-b-B) attached on the web (see Figure 2.9 exact location). Figure 2.28 is a photograph of gage 8 (BA8A 1-c-B, see Figure 2. after completion of wiring. The cables of all the gages at a cross girder were brou to the outside of the trapezoidal girder through existing access holes, as shown Figure 2.29, and into the junction box, Figure 2.30. The junction boxes at the cr girders were specially fabricated for easy connection to the strain recordi instrument, and are water tight when closed for long-term protection and futu measurement of strains. All strain gages inside the box girder were also weath proofed for long-term usage. The connection of gages to the junction box outp sockets are listed in Tables 2.1 to 2.3.

2.2 Recording of Live Load Strains

For the recording of service (traffic) load induced strains, an electrical magnetic tape recorder capable of simultaneous recording of 21 channels was connected through signal conditioners to a junction box. Once the tape was set in motion, all variations of strains at the connected strain gages were recorded, including the effects of vehicular loads, wind, thermal variation, etc.

At the Luling Bridge, the instruments were placed in a van, which was parked in the emergency lane on the bridge deck near a junction box. Figure 2.31 is a photograph showing the general setup.

The recorded strains on a tape can be played back and plotted out as strain versus time data, or fed into a computer for evaluation of the data.

2.3 Procedure of Testing

In order to be able to correlate the strain data and the service loads on the bridge, test trucks of known weight were employed. Two tractor-semitrailers simulation HS20 trucks were arranged by the LaDOTD. Truck No. 1 (159-502, a 3S2) had a gross weight of 80,140 pounds; and truck No. 2 (159-504, a 3S3) 82,180 pounds. Table 2.4 shows the record of axle-group and total weights of these trucks.

The test trucks traveled on the bridge deck either side-by-side (abreast) in two lanes, or in tandem in the traveling lane in both directions (southbound and northbound). Two different speeds of travel were made: crawling at about 5 mph and driving at about 60 mph. These combinations are listed in Tables 2.5, 2.6 and 2.7 for cross girders 5, 4, and 3, respectively. Figures 2.32 and 2.33 are photographs of the test trucks, during one of the test runs, and a regular truck. The test truck runs were all made on November 4, 1986.

Because there were 24 strain gages at cross girder 3 for the 21 channel tape recorder, the gages were divided into two groups. The grouping arrangement for CG5, CG4, and CG3 are listed in Tables 2.8, 2.9, and 2.10, respectively. When strains of gages at cross girder 3 were recorded for the test truck runs, it was already confirmed from the data of cross girders 4 and 5 that the crawl runs and the corresponding speed runs generated almost the same strains. Consequently, only the speed runs of the test trucks were made and repeated for the other two groups of gages.

Besides the recording of strains due to the test trucks, live load strains due to regular traffic were recorded for each grouping at the cross girders. These measurements were acquired on November 3 to November 6, 1986. There was very light traffic throughout the entire period of strain measurement. The estimated average daily truck traffic (ADTT) was only 640 in both directions. After the test truck runs, 21 gages with a relatively higher magnitude of strains were selected and grouped together for further service load strain recording on November 5 and 6, 1986. This grouping arrangement is listed in Table 2.11. Altogether over 15 hours of test records were acquired.

Selected results of strain measurement are presented and discussed in the following section.

3. RESULTS OF STRAIN MEASUREMENTS

3.1 Stress-Time Data from Test Trucks

The recorded strains during the test truck runs were examined visually through a display unit or a plotter. The time variation of strain at a strain gage is an indication of the response of the bridge component at that point. Since strains are directly proportional to stresses in the elastic range of bridge behavior, strain-time records are stress histories.

Figure 3.1 shows the stress-time data of eight locations at cross girder 4. These stresses were induced by the test trucks traveling southbound in tandem in the traveling (west) lane, generally above the west (No. 2) web of the west (BA) trapezoidal box. (See Figure 1.1 for bridge profile and cross section.) Each grid of the horizontal (time) scale is one second. At a truck speed of about 60 mph, this represents about 88 feet of distance of travel. Strain gage 26 and 27 (BA12A 2-a-1 and 2-a-2) were only subjected to stresses when a truck was directly above. Two test trucks induced two excursion of stresses, about 0.3 ksi in compression at gage 26 and less than 0.1 ksi in tension at gage 27. Strain gages 40 and 0 (BA12B 2-b-B and 2-b-T), on the other hand, started to develop stresses when the test trucks came onto the bridge's north side span. Gage 40 was first in compression, underwent live load stress reversals when a truck traveled above, and was then in tension when the second truck crossed over. The range of stress between maximum and minimum was about 1.1 ksi due to these two 80 kip trucks traveling in tandem. Gage 0, at a location below gage 40 and between a drilled hole and a connection opening, had similar stress excursion, but at much lower magnitudes. The other four strain gages also had similar stress-time records.

The response to the test truck runs of the box girder webs at all gaged points can be examined similarly from the stress-time data. These stress-time records are presented in Appendix A, as Figures A1 to A52. The important results obtained from examining and comparing these data are the following.

(A) Effect of Truck Speed

The effect of test truck speed on the induced stresses at the gages was very small, being nondetectable from the stress-time records. Figures 3.2 and 3.3, and Figures 3.4 and 3.5 are examples of corresponding stress-time records. There was no superimposed stress fluctuation due to dynamic effect; and there is no detectable difference in stress magnitudes between the crawl runs and the speed runs of the test trucks. This condition is true of all gages on the box girder webs and the bottom flange.

Therefore, based on the results of test truck runs, it can be said that the effect of truck speed is minimal on the stresses at the retrofit holes in the webs of the trapezoidal boxes.

(B) Effects of Test Truck Combination

Trucks on the trapezoidal box girder of a structure detail induced relatively higher stresses than trucks on the other box girder. Two trucks traveling side by side generated relatively higher stresses than two trucks in tandem. These results are apparent from examining the stress data of Tables 3.1 to 3.6, which summarize the stress range of various truck positions.

Overall, the magnitude of stresses were quite low. The highest stress range was only 1.26 ksi at gage 40 due to two HS20 trucks traveling side by side southbound (Table 3.3).

(C) Effects of Continuous Spans

Because the cable-stayed twin box bridge is essentially a three-span continuous bridge, the structural details at the cross girders are expected to experience live load stress reversal as trucks traverse the bridge. The condition is obvious from examining the stress-time data in Figures 3.1 to 3.23 and Appendix A. It is, therefore, expected that the trapezoidal box girders are subject to alternate "positive bending" and "negative bending" due to truck loads. This is also demonstrated by examining the stress gradient developed in the box girder.

Figure 3.6 shows the stress gradients at the cross section of cross girder 5 with strain gages 47, 49, 52, 53, 54 and 56. The corresponding stress-time data are shown in Figure 3.7. At the instance t_1, the upper portion of the box girder was in

tension while the lower portion was in compression, corresponding to a "negative bending". The test trucks were traveling side by side in the north side span. At time t_2, the stresses were compressive in the upper portion and tensile in the lower portion, corresponding to a "positive bending" and consistent with the truck position at the cross section. The box girder was primarily in vertical bending with little torsion. Figures 3.8 and 3.9 are similar plots for the same cross section, but with the test trucks traveling north on the other box girder. The condition of reversal of stress gradients as well as the domination of vertical bending remained the same. Figures 3.10 to 3.21 show the stress gradients and corresponding stress-time records for other test truck runs at other cross girders. All provide similar results.

This regularity of results from test truck runs provides a solid base for the interpretation of stress data from regular truck traffic.

3.2 Stress Data from Regular Traffic

Two conditions had very strong influence on the stress data obtained from regular truck traffic during the four days of field measurement.

(1) The live load stresses due to trucks were quite low, and

(2) There were very few trucks traveling across the bridge.

The recorded magnitude of maximum, minimum and range of live load stresses due to regular trucks were all below 1 ksi. In fact, most of the stress ranges were well below 1 ksi. Figures 3.22 and 3.23 are stress-time data of some gages produced by several of these trucks. Compared to the corresponding stress-time record from the test trucks, it is obvious that the characteristics of stress variation is the same and the magnitudes are comparable.

The estimated ADTT was 640 in both directions (by LaDOTD). The actual truck traffic during the recording hours was less than a third of this estimate. With such low volume of truck traffic, not much stress data could be recorded. Nevertheless, based on these limited data, stress range frequency diagrams for some gages are compiled. These are gages with relatively higher stress magnitudes from the test truck runs. The frequency diagrams are presented in Figures 3.24 to 3.31. The corresponding tabulation are given in Tables 3.7 to 3.9.

In each of the stress range frequency diagrams, the number of occurrences are plotted against the live load stresses, as bar charts. The general location of the strain gage is sketched below the diagram. For example, gage 46 at BA14A 2-a-T (Channel 7 of cross girder 5, Figure 3.25) was subjected to 18 cycles of stress range between 0.30 and 0.66 ksi, 3 cycles between 0.66 and 1.02 ksi, and 2 and 1 cycle between 1.02-1.38 ksi and 1.38-1.74 ksi, respectively. These data are listed in Table 3.7. Also listed are the equivalent constant amplitude stress ranges (S_{re}) for all stress cycles above the indicated stress range magnitudes.

In all cases (see Tables 3.7 to 3.9), the magnitude of the maximum stress range, the equivalent constant amplitude stress range, and the occurrence frequency are very low.

3.3 Stresses from Unknown Cause

While the magnetic tape recorder was set up for monitoring the strain changes at cross girder 5, a surge of strains was recorded at all gages while there were no trucks on the bridge. The stress-time response of this occurrence are shown in Figure 3.32. These traces do not have the characteristics of the truck-load induced response. Nor can the surge be attributed to electrical noises which have high frequencies. It is speculated that the cause could be from a wind gust or some structural release, at a cable or tie down, or ground motion as it was felt by the team working on the bridge.

Table 3.10 summarizes the stresses produced by this occurrence. The highest stress range was 16.3 ksi at gage 46 (Channel 7, BA14A 2-a-T). The adjacent gage 48 (BA14A 2-a-B in channel 8) experienced 8.41 ksi. Examination of these data and the stress-time traces revealed that all gages except gage 47 (Channel 1, BA14 2-TF) were in tension at the same time. Gages 47 and 49 (Channels 1 and 2, BA14 2-TF and BA14 2-MD) had a minor reversal of stress. All these gages were at one cross section (see Figure 2.21). Without simultaneous stress records from cross girders 3 and 4, a more detailed examination cannot be made. [Although it could be further speculated that the cable at CG5 on the west side pulled the cross girder and generated tension in the box girder, particularly at BA14A 2-a beyond the cross girder.

Gage 47 (BA14-2-TF) was above the cross girder and was subjected to compression.]

No other incident of this nature was observed during this four day study.

4. RESIDUAL CRACK AT CROSS GIRDER CONNECTIONS

4.1 Crack Characteristics

There were several retrofit holes where the crack in the trapezoidal box girder web was not completely removed by the hole. There existed uncracked ligaments between the retrofit holes and the edges of plates to be evaluated. A number of these locations were identified in References 1 and 2.

The strain gages installed in the west box girder at cross girders 3, 4 and 5 permitted an assessment of the maximum stress range at these locations. Although no measurement of stresses was obtained at other cross girder locations, the stress magnitudes obtained at CG 3, 4 and 5 will be comparable to those at CG10, 9 and 8, respectively. (See Figure 1.1.)

Table 4.1 provides a summary of the applicable detail and core locations as well as the strain gage numbers at these locations.

Figure 4.1 shows the uncracked ligament at CG9 Unit BA22B, detail 2-a-B. The core removed from this location can be seen in Figure 4.2. At CG10, unit BA26B, two distinct uncracked ligaments can be seen at Detail 1-a-B, in Figure 4.3.

At cross-girder 5 (CG5), only one core was available to define the crack front. Figure 4.4 shows the edge crack extending into the web plate from the inside surface. No other defined crack fronts were available from CG5. The field measurement results would be applicable to CG8.

At CG4 unit BA12A, two cores were removed from Detail 1-a-T, as seen in Figure 2.15. Core 2 contained the crack tip, as shown schematically in Figure 4.5 The exposed surface of the crack tip in Core 2 can be seen in Figure 4.6. Core 3 adjacent to the re-entrant corner of this joint had a small uncracked ligament near the outside surface of the web, as shown in Figure 4.7. At Detail 2-a-T of unit BA12A, an uncracked ligament also was apparent from Core 4, as illustrated in Figure 4.8. Figures 4.9 and 4.10 show the crack conditions in Unit BA12B at Details 1-a-B and 2-a-B. At the Core 1′ adjacent to Detail 1-a-B, edge cracks can be seen on each side of the uncracked center ligament. The crack tip was 0.95 inches from the outside

surface and 1.16 inches from the inside surface, providing near symmetrical edge cracks. Figure 4.10 shows that core 5′ has an embedded crack with a small (0.14 inches) ligament on the inside edge. The total crack length is 1.04 inches.

At cross-girder CG3, only three of the five cores contained cracks. As a result, the uncracked residual ligaments were not defined at Details 1-a-B and 2-a-T in Unit BA8A. Figures 4.11, 4.12 and 4.13 show the crack fronts at the retrofit hole for Details 1-b-T, 1-b-B, and 1-c-B.

The field inspections in 1986 indicated that the residual cracks had not extended as a result of the cyclic loading to that time.

4.2 Crack Growth Predictions

Among the details listed in Table 4.1, the most severe crack extension characteristics occur at cross girder CG4, where the largest stress ranges observed were at Details BA12B 1-a-B and 2-a-B (gages 41 and 43). The maximum measured stress range occurred when two HS20 vehicles crossed the span side by side. The stress range was 0.74 ksi at gage 41, and 0.64 ksi at gage 43.

At BA12B 2-a-B, an embedded crack existed, as illustrated in Figure 4.10. The possibility of crack extension at the smaller ligaments was examined assuming an embedded crack model [3].

$$\Delta K = S_r \sqrt{\pi a} \left[\sec \left(\frac{\pi a}{2w} \right) \right]^{1/2} \qquad (1)$$

where ΔK = stress intensity range, ksi $\sqrt{\text{in.}}$

S_r = stress range, ksi

a = half the embedded crack length, in.

w = distance from the center of the crack to the edge of the plate, in.

At Detail 2-a-B, with S_r = 0.74 ksi, a = 0.52 in. and W = 0.66 in., Eq. 1 provided:

$$\Delta K = 0.74 \sqrt{\pi\ (0.52)} \left[\sec\left(\frac{\pi\ (0.52)}{1.32}\right)\right]^{1/2} \qquad (1)$$
$$= 1.66\ ksi\sqrt{in}\ . < \Delta K_{th} = 2.75\ ksi\sqrt{in}\ .$$

This indicated that crack extension was not likely to occur at this crack under this peak stress range condition. The predicted stress intensity factor was well below the crack growth threshold, ΔK_{th}[3][4]. Hence, no crack extension would be predicted. The magnitude of the crack growth threshold, ΔK_{th} = 2.75 ksi$\sqrt{in}$. corresponds to a worst case assumption. It assumes that large residual tensile stress from weld restraint still exists at the crack tip.

At Detail BA12B 1-a-B, the crack was more severe as the edge cracks were larger. The edge crack model used was [3]

$$\Delta K = 1.12\ S_r \left[2w \tan \frac{\pi a}{2w}\right]^{1/2} \qquad (2)$$

at Detail 1-a-B, S_r = 0.64 ksi, a = 1.16 in. and w = 1.36 in.. Hence,

$$\Delta K = 1.94\ ksi\sqrt{in}\ . < \Delta K_{th}$$

Again, crack extension was not likely.

The information available indicates that under traffic conditions, cyclic stresses in the trapezoidal box units are not likely to exceed the crack growth threshold. The maximum stress range in the box girder units varied from 0.1 ksi to 0.74 ksi at the a, b, and c details with cracks. None of the existing cracks are likely to extend under these conditions. Additional measurements should await completion of the connecting roadways, so that higher frequency truck traffic will occur and a larger number of stress cycles be allowed to accumulate.

5. CONCLUSIONS

Based on the results of field measurements of stresses at the retrofit holes in the trapezoidal box girders, the following summary can be made.

(A) The live load stresses due to test trucks were low. Two simulated HS20 trucks traveling side by side generated the highest live load stress range of 1.32 ksi at a retrofit hole. The maximum and minimum stress was 0.54 and -0.78 ksi, respectively. Most of the 59 strain gages had maximum stress range levels well below 1.0 ksi from the test trucks.

(B) There was very little impact or dynamic effect from the test vehicles. Trucks traveling at crawl speed generated practically the same stress magnitudes as trucks traveling at 60 mph.

(C) There was only light traffic on the bridge. During the period of stress measurement, the regular traffic trucks generated maximum stress magnitudes comparable to those developed by the test trucks.

(D) By using the measured stress magnitudes and the actual dimensions of cracks at the retrofit holes, it was determined that none of the existing cracks are likely to propagate under the current traffic conditions.

(E) An unknown cause, possibly a wind gust and structural release, produced one excursion of relatively high stresses at the strain gages being monitored at CG5. The maximum stress range was 16.3 ksi at a single retrofit hole. This type of event only occurred once during the duration of these studies.

6. RECOMMENDATIONS

From these results, the following recommendations are suggested.

(A) Additional measurements of live load stress should be made when the connecting roadways have been completed. More trucks will likely induce higher magnitudes of stresses and higher frequencies of occurrences.

(B) Consideration should be given to continuous monitoring of stresses at a few retrofit holes for an extended period of time (at least two weeks). This will provide more information on live load stresses generated by all causes, including truck traffic, wind loads, and all other conditions. It is recommended that these measurements be carried out in 1996.

(C) Routine inspection of the retrofit holes should be continued at normal inspection intervals covered by the biannual inspections. There is no reason for more frequent examination as long as the truck traffic frequency remains low (i.e. less than 1000 ADTT).

7. REFERENCES

1. Fisher, J. W. and Pense, A. W., "An Evaluation of the Cracking in the Luling Bridge Box Girder Webs and Recommendations for its Retrofit", Fisher, Fang & Associates, April 1982.

2. Fisher, J. W. and Pense, A. W., Letter report to Louis A. Garrido, October 3, 1983.

3. Fisher, J. W., Fatigue and Fracture in Steel Bridges, John Wiley, 1984.

4. Barson, J. M. and Rolfe, S. T., Fracture and Fatigue Control in Structures, 2nd Ed., Prentice-Hall, Inc., 1987.

8. TABLES

Table 2.1
STRAIN GAGE IDENTIFICATION AT CG3

Luling Bridge
Gages at Cross-Girder 3

Identification	Gage No.	Box Output
BA8 B 1-b-B	1	1
B 1-b-T	2	2
B 1-a-B	3	3
B 2-b-T	4	4
B 2-b-B	5	5
B 2-a-B	6	6
B 2-c-B	7	7
B 1-c-B	8	8
B 2-d-B	9	9
B 1-d-B	10	10
A 2-d-T	11	11
A 2-b-B	12	13
A 2-b-T	13	14
A 2-a-T	14	15
2-TF	15	16
A 2-c-B	16	22
2-BF	17	17
A 1-d-T	18	12
A 1-a-T	20	18
A 1-b-T	21	23
A 1-b-B	22	24
1-TF	23	19
A 1-c-B	24	21
1-BF	25	20

Table 2.2
STRAIN GAGE IDENTIFICATION AT CG4

Luling Bridge
Gages at Cross-Girder 4

Identification	Gage No.	Box Output
BA12 A 2-a-1	26	1
A 2-a-2	27	2
A 2-a-3	28	3
A 2-a-4	29	4
A 2-c-T	30	6
A 2-b-B	31	5
A 2-d-T	32	10
B 2-d-B	33	11
A 1-b-B	34	7
A 1-a-B	35	8
A 1-c-B	36	9
A 1-d-T	37	12
B 1-d-B	38	13
B 2-a-T	39	14
B 2-b-B	40	16
B 2-a-B	41	15
B 1-b-T	42	19
B 1-a-B	43	20
B 1-c-B	44	21
B 2-c-B	45	18
B 2-b-T	0	17

Table 2.3
STRAIN GAGE IDENTIFICATION AT CG5

Luling Bridge
Gages at Cross-Girder 5

Identification	Gage No.	Box Output
BA14 A 2-a-T	46	7
2-TF	47	1
A 2-a-B	48	8
2-MD	49	2
B 2-d-B	50	13
B 1-d-B	51	14
2-BF	52	3
1-TF	53	4
1-MD	54	5
A 1-a-B	55	9
1-BF	56	6
B 2-a-T	57	10
B 2-a-B	58	11
B 1-a-B	59	12

Table 2.5
TEST TRUCK RUNS, CG5

Run No.	Lane Location Traveling	Lane Location Passing	Speed (Mph)[2]	Direction	Remarks
1	2[1]	1[1]	5	SB	Abreast
2	1	2	5	NB	Abreast
3	2	1	60	SB	Abreast
4	1	2	60	NB	Abreast
5	2	1	60	SB	Abreast
6	1	2	60	NB	Abreast
7	1/2	-	5	SB	In Tandem[3]
8	2/1	-	5	NB	In Tandem[3]
9	2/1	-	60	SB	In Tandem[3]
10	2/1	-	60	NB	In Tandem[3]
11	2/1	-	60	SB	In Tandem[3]
12	2/1	-	60	NB	In Tandem[3]

(1) Truck No. 1,352, 80.14K
Truck No. 2,353, 82.18K

(2) Approximate Speed

(3) Approximately 500 ft. apart for Run No. 7 and 150 ft. apart for Runs 8 to 12

Table 2.5
TEST TRUCK RUNS, CG5

Run No.	Lane Location Traveling	Passing	Speed (Mph)[2]	Direction	Remarks
1	2[1]	1[1]	5	SB	Abreast
2	1	2	5	NB	Abreast
3	2	1	60	SB	Abreast
4	1	2	60	NB	Abreast
5	2	1	60	SB	Abreast
6	1	2	60	NB	Abreast
7	1/2	-	5	SB	In Tandem[3]
8	2/1	-	5	NB	In Tandem[3]
9	2/1	-	60	SB	In Tandem[3]
10	2/1	-	60	NB	In Tandem[3]
11	2/1	-	60	SB	In Tandem[3]
12	2/1	-	60	NB	In Tandem[3]

(1) Truck No. 1,352, 80.14K
Truck No. 2,353, 82.18K

(2) Approximate Speed

(3) Approximately 500 ft. apart for Run No. 7 and 150 ft. apart for Runs 8 to 12

Table 2.6
TEST TRUCK RUNS, CG4

Run No.	Lane Location Traveling	Passing	Speed (Mph)[2]	Direction	Remarks
1	1[1]	2[1]	5	SB	Abreast
2	2	1	5	NB	Abreast
3	1	2	60	SB	Abreast
4	2	1	60	NB	Abreast
5	1	2	60	SB	Abreast
6	2	1	60	NB	Abreast
7	2/1	-	5	SB	In Tandem[3]
8	2/1	-	5	NB	In Tandem[3]
9	2/1	-	60	SB	In Tandem[3]
10	2/1	-	60	NB	In Tandem[3]
11	2/1	-	60	SB	In Tandem[3]
12	2/1	-	60	NB	In Tandem[3]

(1) Truck No. 1,352, 80.14K
Truck No. 2,353, 82.18K

(2) Approximate speed

(3) Approximately 150 ft. apart

Table 2.7
TEST TRUCK RUNS, CG3

Run No.	Lane Location Traveling	Lane Location Passing	Speed (Mph)[2]	Direction	Remarks
1	1[1]	2[1]	60	SB	Abreast
2	2	1	60	NB	Abreast
3	1	2	60	SB	Abreast
4	2	1	60	NB	Abreast
5	2/1	-	60	SB	In Tandem[3]
6	2/1	-	60	NB	In Tandem[3]
7	2/1	-	60	SB	In Tandem[3]
8	2/1	-	60	NB	In Tandem[3]
9	1	2	60	SB	Abreast
10	2	1	60	NB	Abreast
11	1	2	60	SB	Abreast
12	2	1	60	NB	Abreast
13	2/1	-	60	SB	In Tandem[3]
14	2/1	-	60	NB	In Tandem[3]
15	2/1	-	60	SB	In Tandem[3]
16	2/1	-	60	NB	In Tandem[3]

(1) Truck No. 1,352, 80.14K
Truck No. 2,353, 82.18K

(2) Approximate speed

(3) Approximately 150 ft. apart, except Run No. 7 (200 ft. apart)

Table 2.8
STRAIN GAGE GROUPING, CG5

Grouping Arrangement of Gages at CG5

Channel	Gage No.	Gage ID
1	47	BA14 2-TF
2	49	BA14 2-MD
3	52	BA14 2-BF
4	53	BA14 1-TF
5	54	BA14 1-MD
6	56	BA14 1-BF
7	46	BA14 A 2-a-t
8	48	BA14 A 2-a-B
9	55	BA14 A 1-a-B
10	57	BA14 B 2-a-T
11	58	BA14 B 2-a-B
12	59	BA14 B 1-a-B
13	50	BA14 B 2-d-B
14	51	BA14 B 1-d-B

Table 2.9
STRAIN GAGE GROUPING, CG4

Grouping Arrangement of Gages at CG4

Channel	Gage No.	Gage ID
1	26	BA12 A 2-a-1
2	27	BA12 A 2-a-2
3	28	BA12 A 2-a-3
4	29	BA12 A 2-a-4
5	31	BA12 A 2-b-B
6	30	BA12 A 2-c-T
7	34	BA12 A 1-b-B
8	35	BA12 A 1-a-B
9	36	BA12 A 1-c-B
10	32	BA12 A 2-d-T
11	33	BA12 B 2-d-B
12	37	BA12 A 1-d-T
13	38	BA12 B 1-d-B
14	39	BA12 B 2-a-T
15	41	BA12 B 2-a-B
16	40	BA12 B 2-b-B
17	0	BA12 B 2-b-T
18	45	BA12 B 2-c-B
19	42	BA12 B 1-b-T
20	43	BA12 B 1-a-B
21	44	BA12 B 1-c-B

Table 2.11
STRAIN GAGE GROUPING FOR REGULAR TRAFFIC

Grouping Arrangement of Gages for Regular Traffic

Channel	Gage #	Location	ID
1	2		BA8 B 1-b-T
2	14	CG3	BA8 A 2-a-T
3	20		BA8 A 1-a-T
4	26		BA12 A 2-a-1
5	27		BA12 A 2-a-2
6	28		BA12 A 2-a-3
7	29		BA12 A 2-a-4
8	34		BA12 A 1-b-B
9	35	CG4	BA12 A 1-a-B
10	36		BA12 A 1-c-B
11	33		BA12 B 2-d-B
12	37		BA12 A 1-d-T
13	41		BA12 B 2-a-B
14	43		BA12 B 1-a-B
15	46		BA14 A 2-a-T
16	47		BA14 2TF
17	50		BA14 B 2-d-B
18	48	CG5	BA14 A 2-a-B
19	52		BA14 2 BF
20	58		BA14 B 2-a-3
21	59		BA14 B 1-a-B

Table 3.1
STRESS RANGE (KSI) INDUCED BY TEST TRUCKS SIDE BY SIDE CG5

CG5 Gage No.	Test Trucks Side by Side Southbound	Northbound
46	0.19	0.09
47	0.41	0.26
48	0.16	0.08
49	0.23	0.16
50	0.61	0.51
51	0.65	0.46
52	0.67	0.50
53	0.42	0.38
54	0.27	0.20
55	0.04	0.08
56	0.64	0.51
57	0.33	0.08
58	0.57	0.45
59	0.57	0.36

Table 3.2
STRESS RANGE (KSI) INDUCED BY TEST TRUCKS IN TANDEM CG5

CG5 Gage No.	Test Trucks in Tandem Southbound	Northbound
46	0.15	0.09
47	0.24	0.15
48	0.12	0.07
49	0.16	0.15
50	0.42	0.33
51	0.39	0.33
52	0.40	0.36
53	0.26	0.23
54	0.15	0.17
55	0.06	0.06
56	0.36	0.36
57	0.30	0.07
58	0.38	0.27
59	0.30	0.22

Table 3.3
STRESS RANGE (KSI) INDUCED BY TEST TRUCKS SIDE BY SIDE CG4

CG4 Gage No.	Test Trucks Side by Side Southbound	Northbound
26	0.43	0.27
27	0.08	0.04
28	0.32	0.10
29	0.20	0.15
30	0.33	0.15
31	0.18	0.15
32	0.25	0.14
33	0.81	0.57
34	0.08	0.15
35	0.16	0.23
36	0.11	0.18
37	0.22	0.31
38	0.78	0.66
39	0.14	0.07
40	1.26	0.90
41	0.74	0.51
42	0.54	0.39
43	0.63	0.36
44	0.90	0.51
45	0.83	0.57
0	0.48	0.24

Table 3.4
STRESS RANGE (KSI) INDUCED BY TEST TRUCKS IN TANDEM CG4

CG4 Gage No.	Test Trucks in Tandem Southbound	Northbound
26	0.27	0.12
27	0.07	0.02
28	0.30	0.04
29	0.13	0.09
30	0.30	0.06
31	0.13	0.08
32	0.15	0.08
33	0.66	0.36
34	0.04	0.08
35	0.12	0.12
36	0.04	0.12
37	0.09	0.16
38	0.48	0.45
39	0.10	0.06
40	1.05	0.48
41	0.56	0.30
42	0.47	0.21
43	0.48	0.21
44	0.66	0.30
45	0.57	0.36
0	0.39	0.15

9. FIGURES

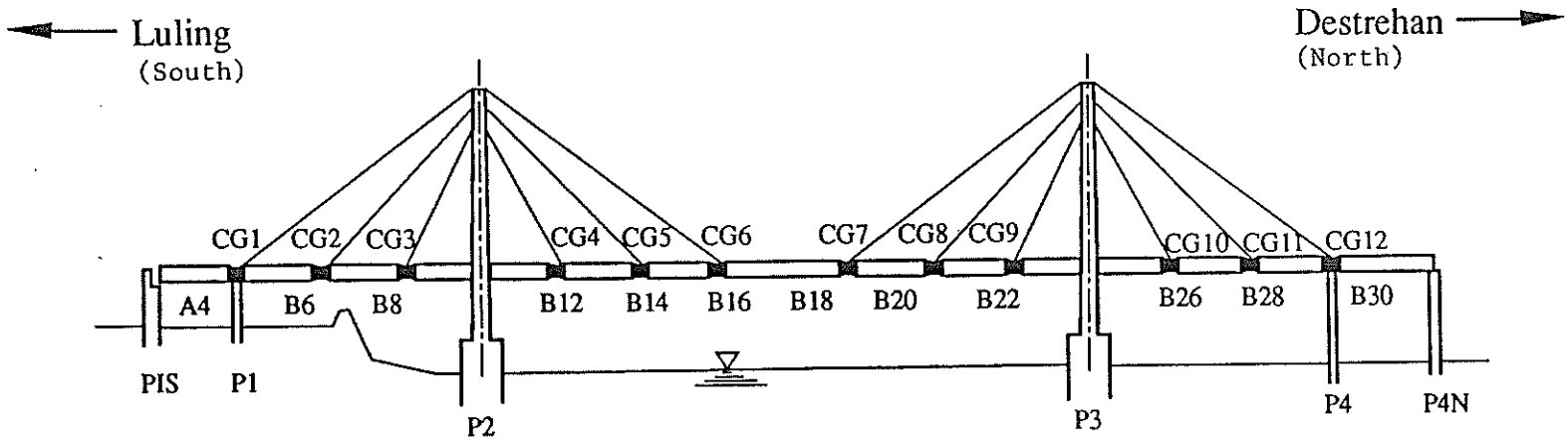

CG = Cross Girder
B = Block Number

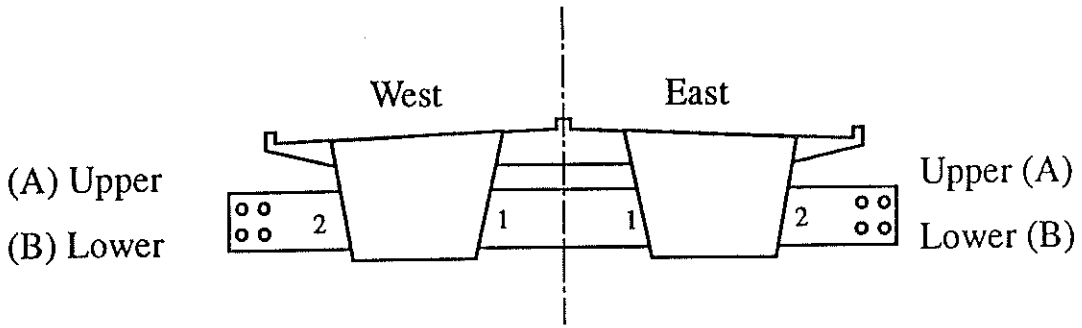

Figure 1.1. Profile and cross section of bridge.

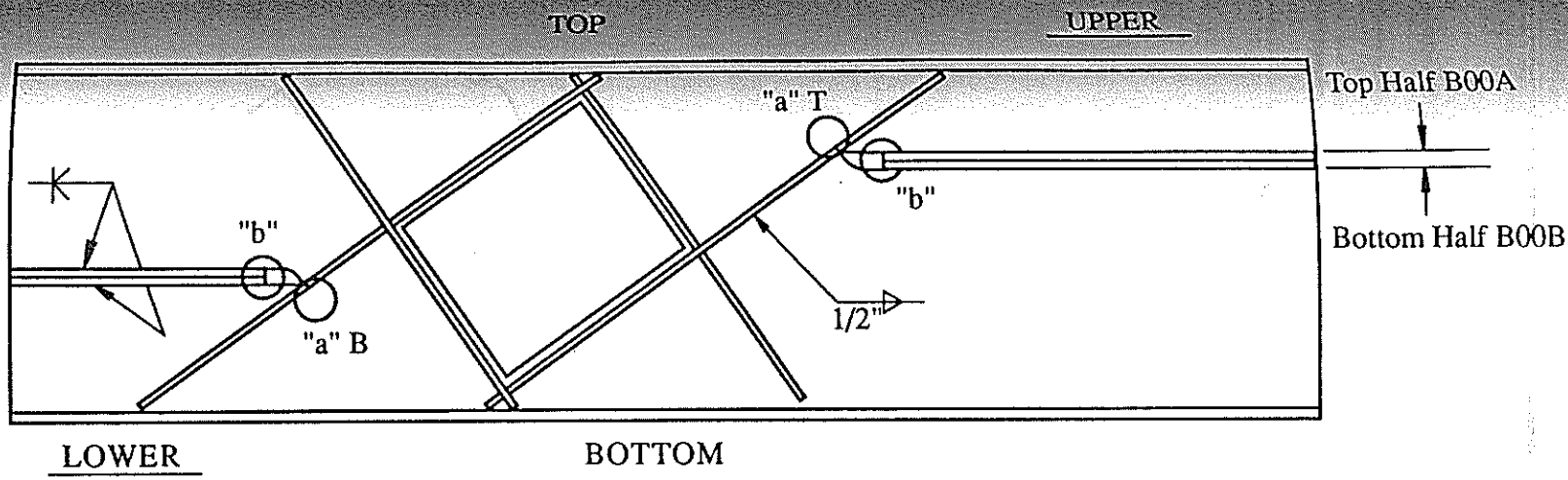

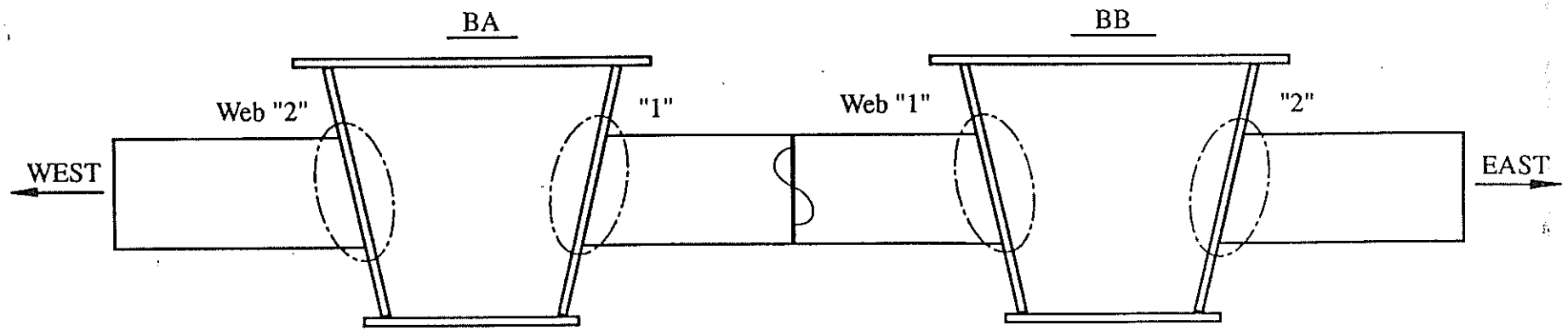

Figure 1.2. Identification of locations.

Luling Bridge
11/4/86 Tape II
Test Trucks in Tandem, Speed Run, 5B
CG 5, All Gages Fs 25

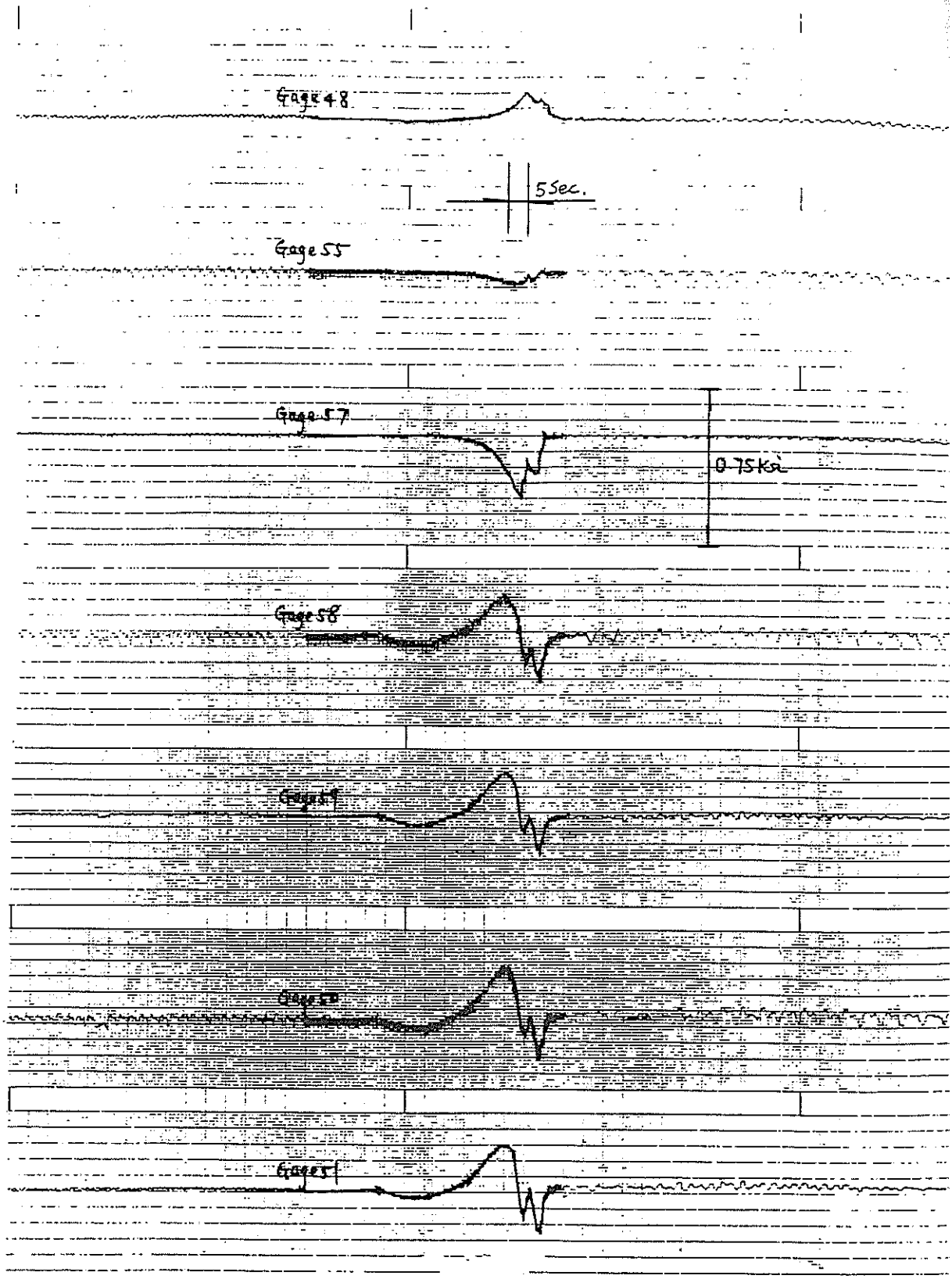

Figure A14

Luling Bridge
11/4/86 Tape II
Test Trucks in Tandem, Speed Run, SB
CG5, All Gages FS 25

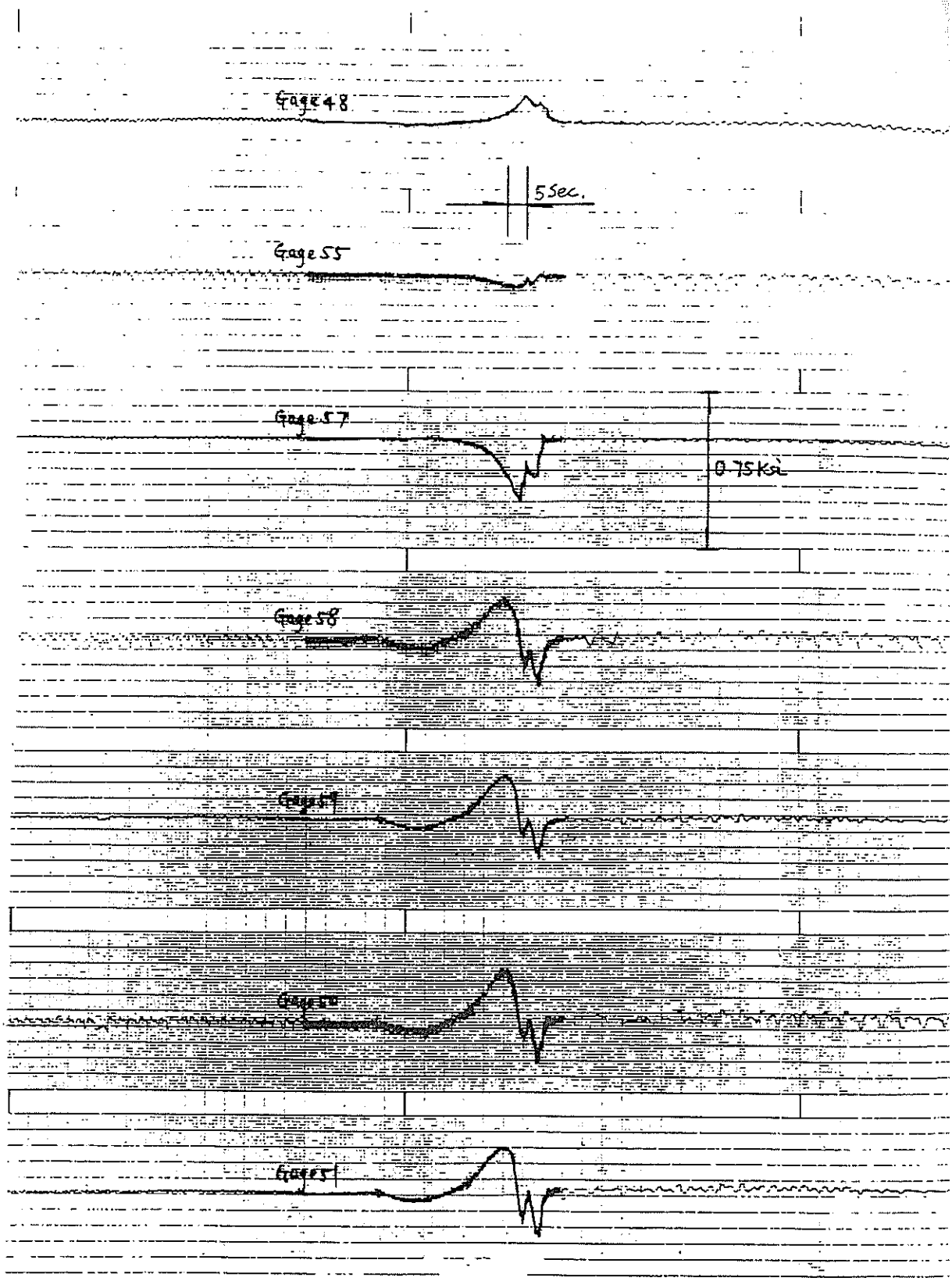

Figure A14

Luling Bridge
11/4/86 Tape II
Test Trucks in Tandem, Speed Run, SB
CG 5, All Gages FS 25

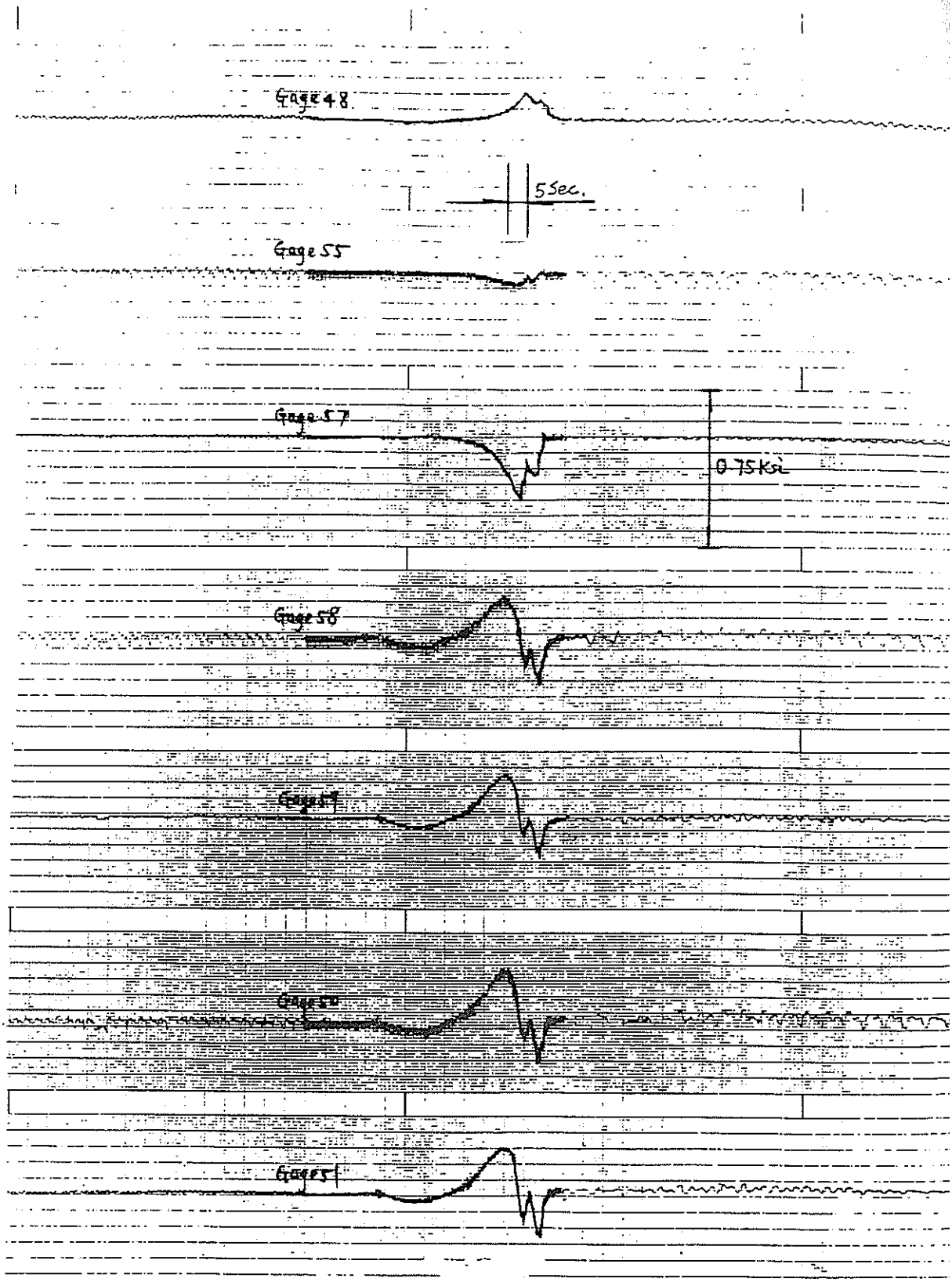

Figure A14

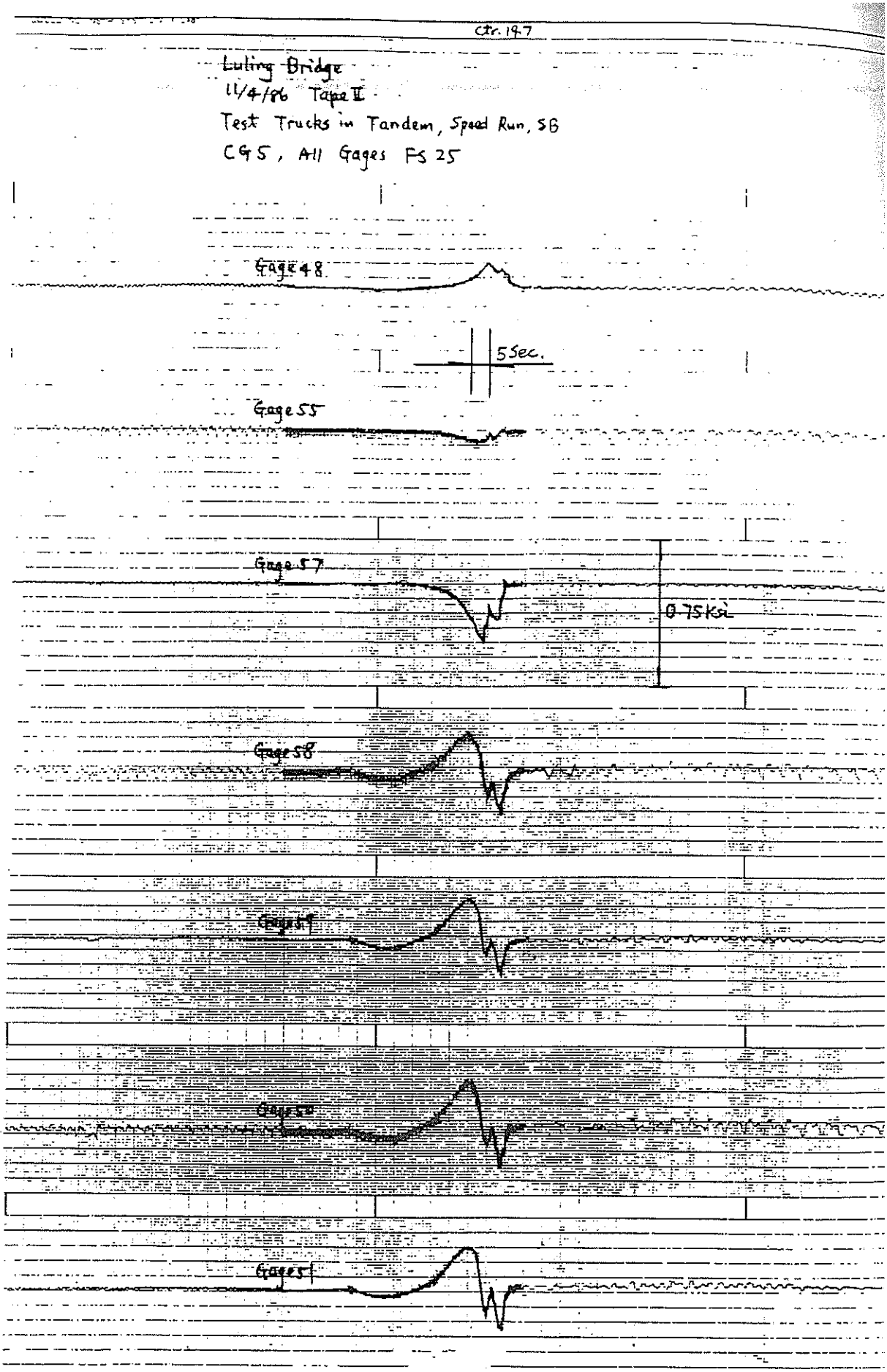
Luling Bridge
11/4/86 Tape II
Test Trucks in Tandem, Speed Run, SB
C45, All Gages FS 25
Gage 48
5 Sec.
Gage 55
Gage 57
0.75 Ksi
Gage 58
Gage 47
Gage 50
Gage 51

Figure A14

Luling Bridge
11/4/86 Tape II
Test Trucks in Tandem, Speed Run, SB
CG 5, All Gages FS 25

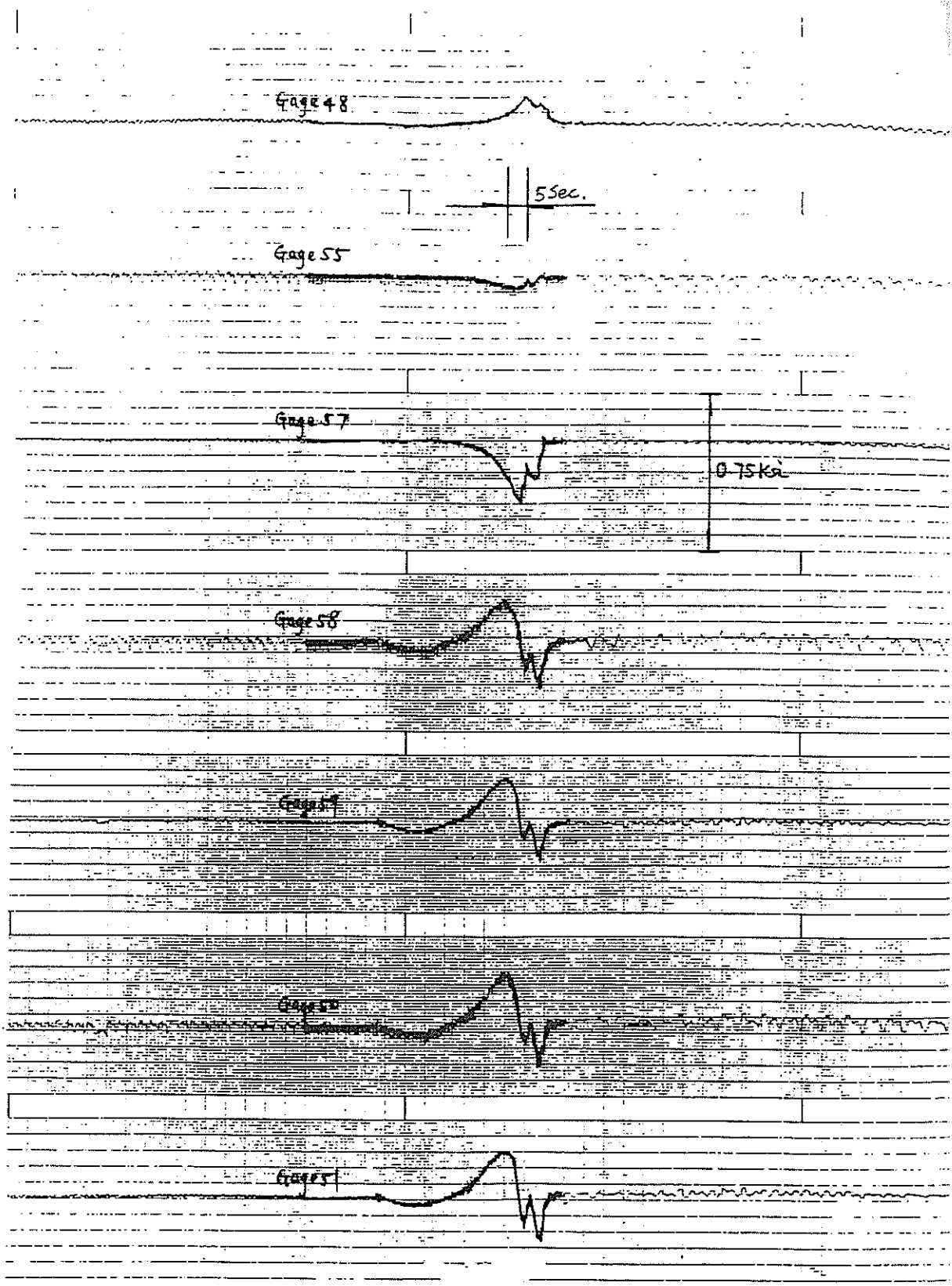

Figure A14

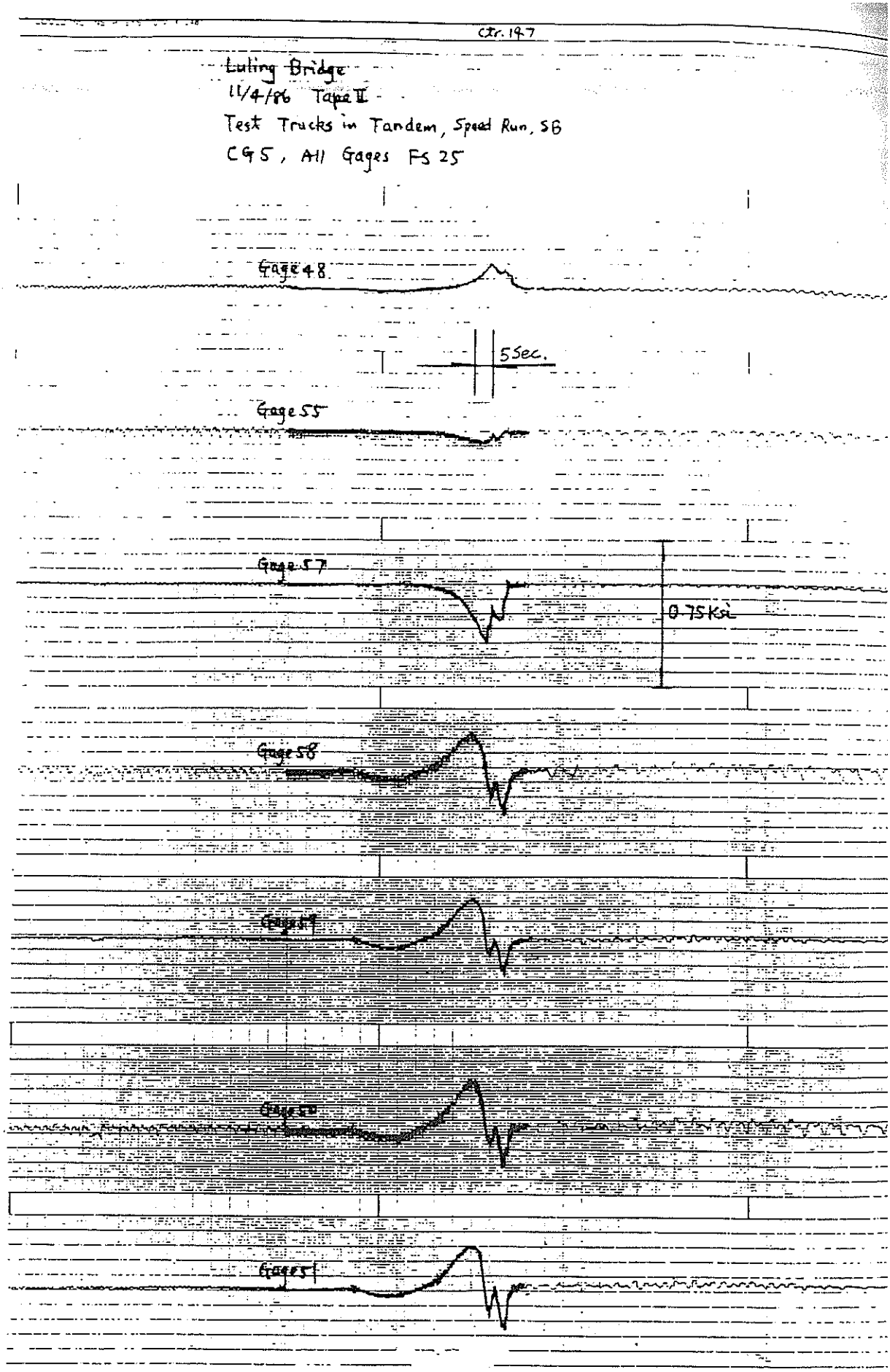
Luling Bridge
11/4/86 Tape II
Test Trucks in Tandem, Speed Run, SB
CG 5, All Gages FS 25
Gage 48
5 Sec.
Gage 55
Gage 57
0.75 Ksi
Gage 58
Gage 59
Gage 60
Gage 51

Figure A14

Luling Bridge
11/4/86 Tape II
Test Trucks in Tandem, Speed Run, 56
CGS, All Gages FS 25

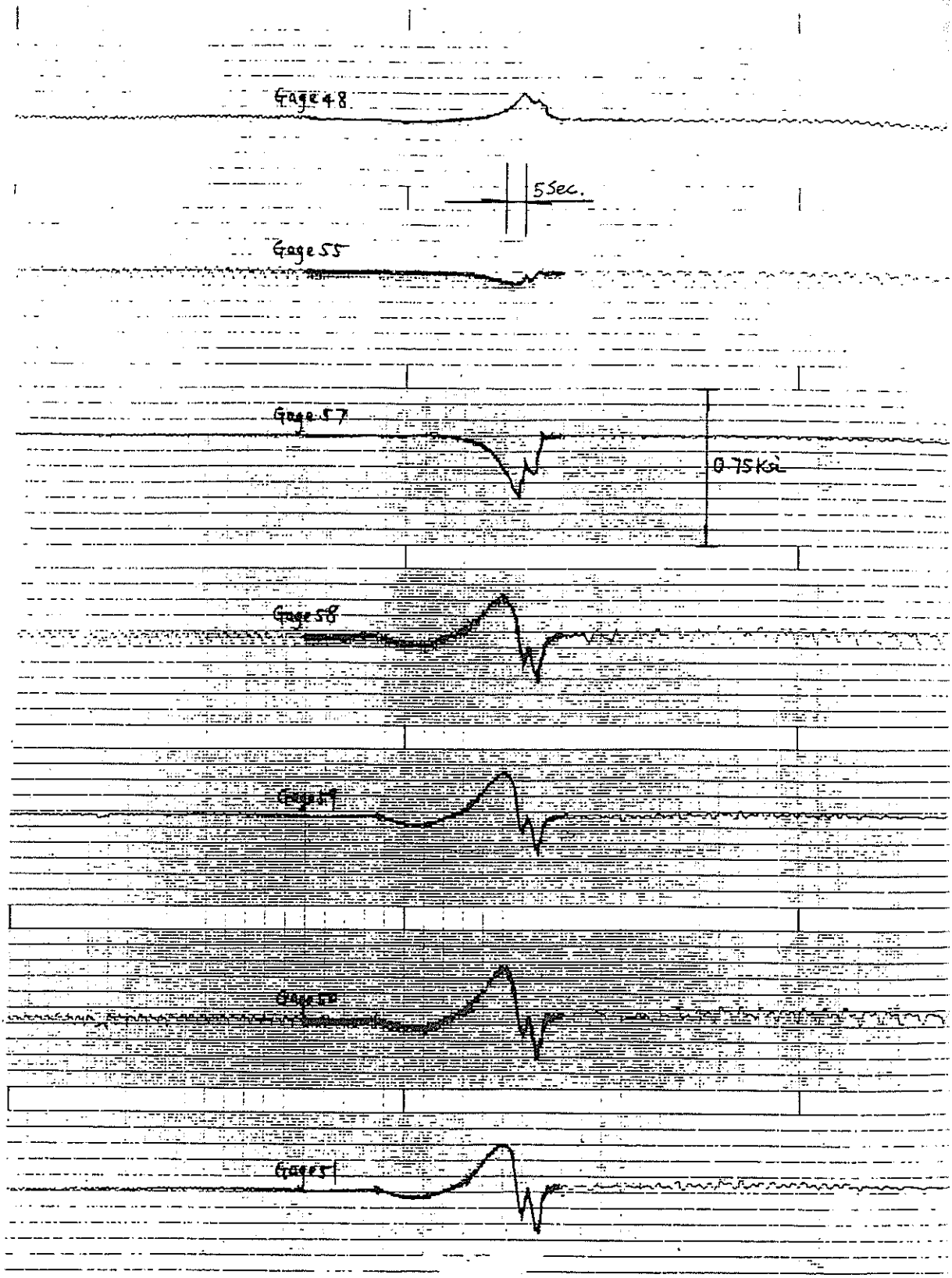

Figure A14

Luling Bridge
11/4/86 Tape II
Test Trucks in Tandem, Speed Run, SB
C95, All Gages FS 25

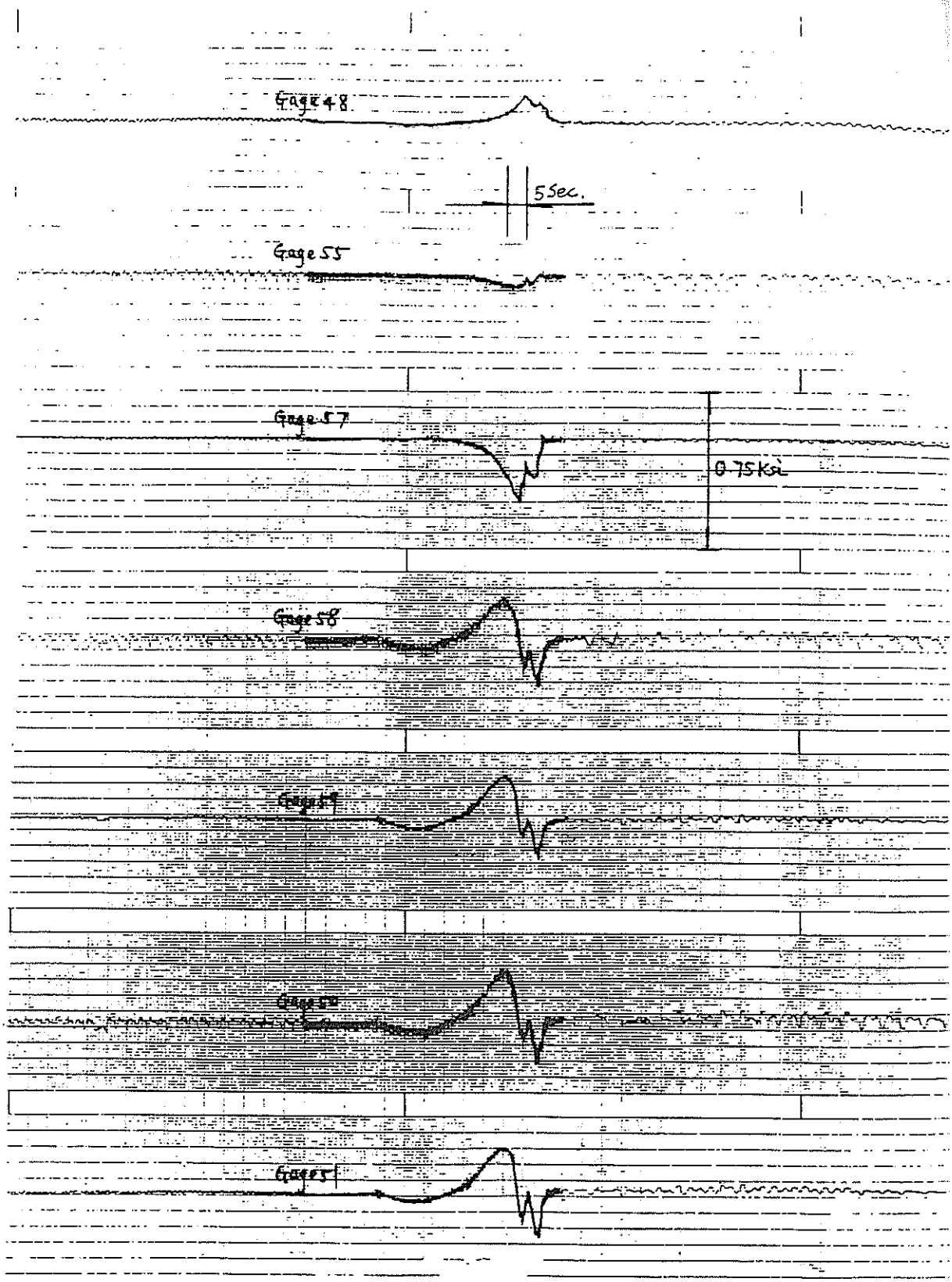

Figure A14

Luling Bridge
11/4/86 Tape II
Test Trucks in Tandem, Speed Run, SB
CG 5, All Gages FS 25

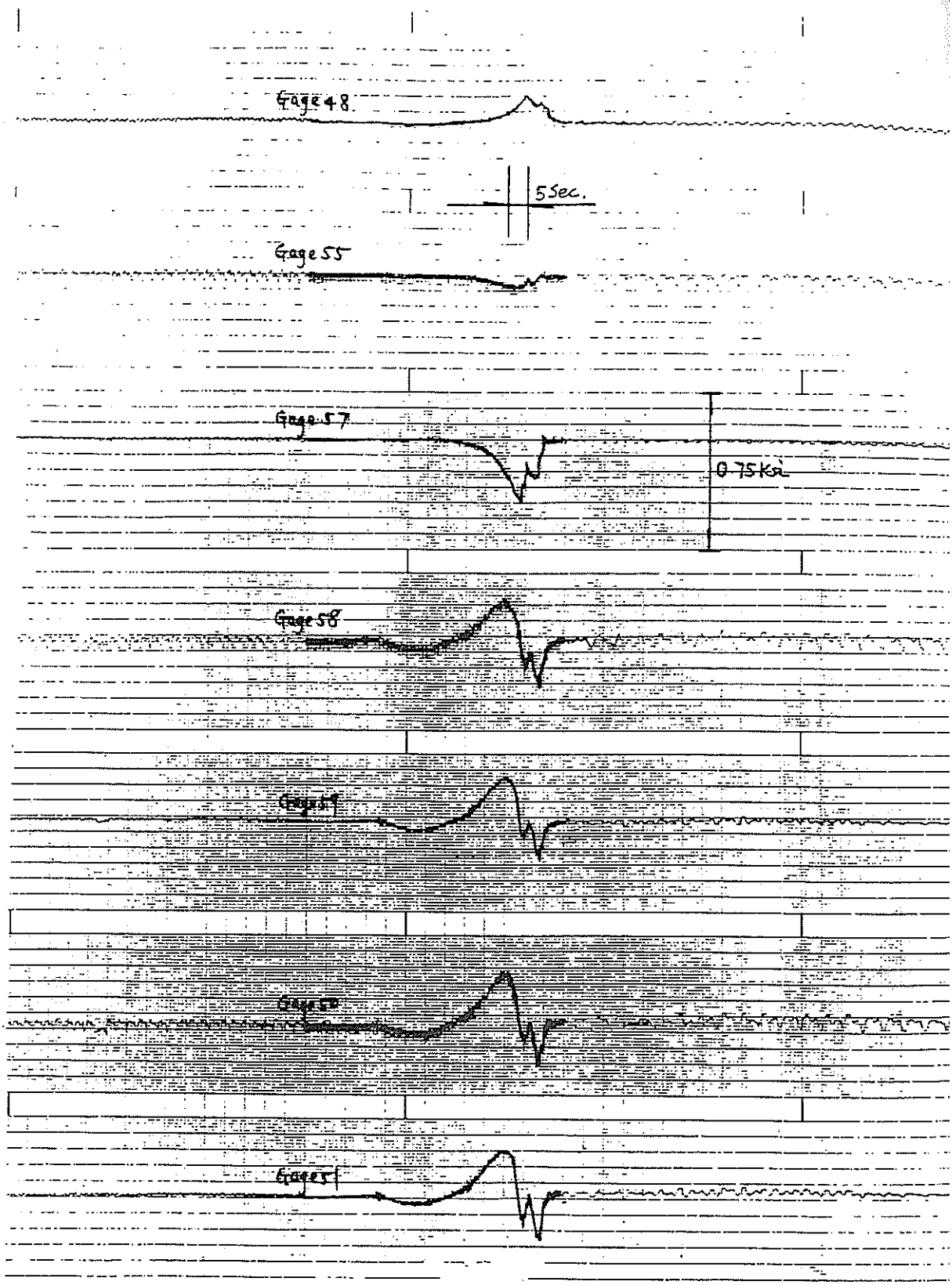

Figure A14

Luling Bridge
11/4/86 Tape II
Test Trucks in Tandem, Speed Run, SB
CG5, All Gages Fs 25

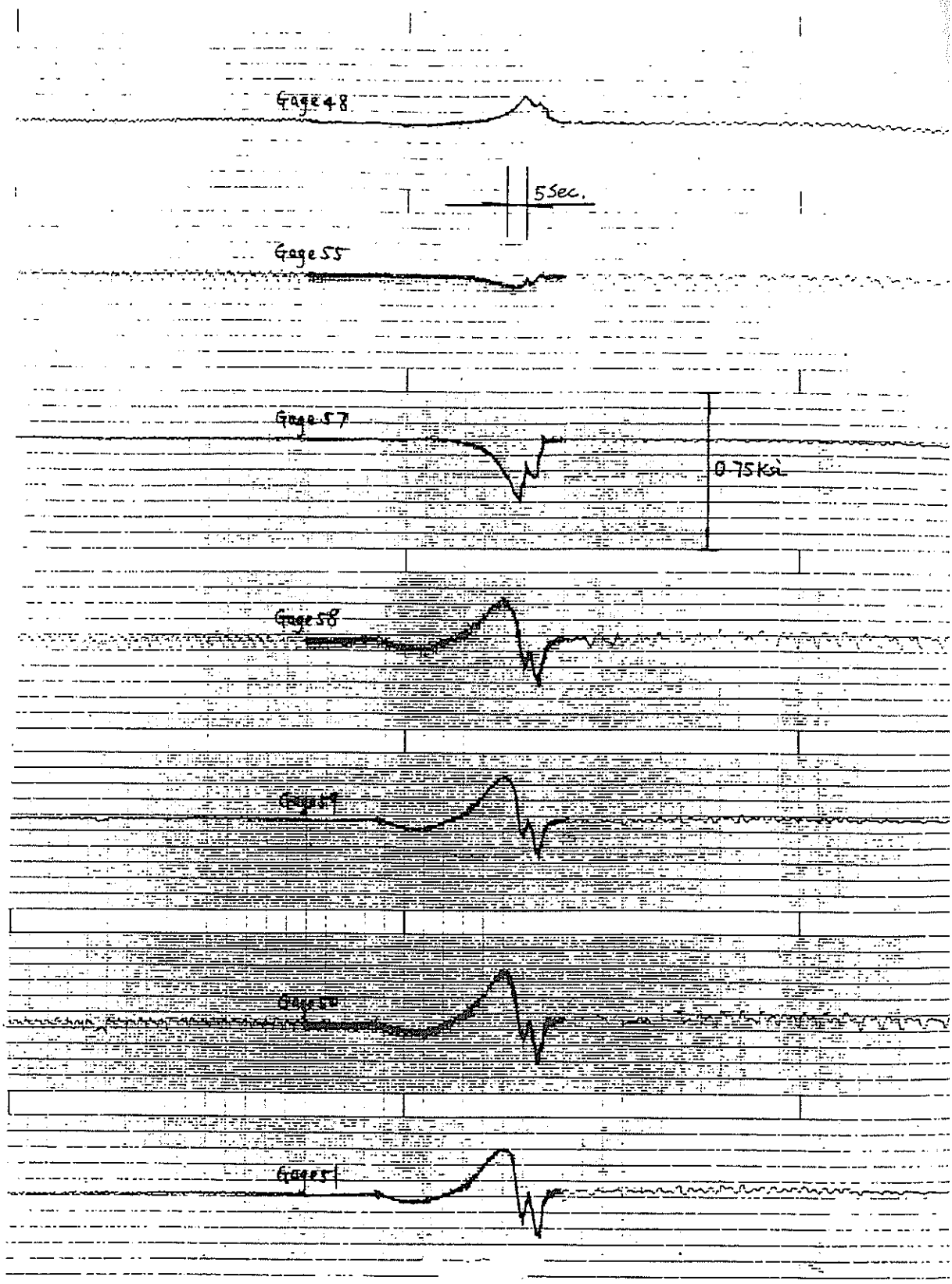

Figure A14